

# Crystal Structure of the Human Laminin Receptor Precursor\*<sup>§</sup>

Received for publication, October 31, 2007, and in revised form, November 13, 2007  
Published, JBC Papers in Press, December 6, 2007, DOI 10.1074/jbc.C700206200

Kelly V. Jamieson<sup>‡</sup>, Jinhua Wu<sup>§</sup>, Stevan R. Hubbard<sup>§1</sup>,  
and Daniel Meruelo<sup>‡2</sup>

From the <sup>‡</sup>Gene Therapy Center, Cancer Institute and Department of Pathology, New York University School of Medicine, New York, New York 10016 and the <sup>§</sup>Structural Biology Program, Kimmel Center for Biology and Medicine of the Skirball Institute, and Department of Pharmacology, New York University School of Medicine, New York, New York 10016

The human laminin receptor (LamR) interacts with many ligands, including laminin, prions, Sindbis virus, and the polyphenol (–)-epigallocatechin-3-gallate (EGCG), and has been implicated in a number of diseases. LamR is overexpressed on tumor cells, and targeting LamR elicits anti-cancer effects. Here, we report the crystal structure of human LamR, which provides insights into its function and should facilitate the design of novel therapeutics targeting LamR.

The human LamR<sup>3</sup> precursor protein and the p40 ribosomal protein are encoded by the same gene (*37LRP/p40*) (1), demonstrating that human LamR is a protein that has acquired dual function through evolution, acting as both a cell surface receptor and a ribosomal protein (2). In addition to its role as a ribosomal protein, LamR is a nonintegrin cell surface protein that has been identified as the receptor for the extracellular matrix molecule laminin-1 (3), pathogenic prion protein (4), Sindbis virus (5), Venezuelan equine encephalitis virus (6), cytotoxic necrotizing factor types I and II (7), and adeno-associated virus serotypes 2, 3, 8, and 9 (8). At the cell surface, LamR exists as a

monomer (37 kDa) and dimer (67 kDa) (4). The homo- or heterodimeric state of 67-kDa LamR has yet to be resolved, but its association with the cell surface is mediated by fatty acid acylation (9). LamR expression acts as a prognostic factor in determining the degree of malignancy of human cancer patients (10). Overexpression of LamR correlates with a highly invasive cell phenotype and increased metastatic ability (10), mediated by the high affinity binding between LamR and laminin in the extracellular matrix. The dual function of human LamR as a receptor at the cell surface and as a component of the translational machinery may be important for understanding how overexpression of LamR in cancer affects disease pathogenesis.

The role of LamR as a ribosomal protein is also of significant interest. Intracellular LamR is localized on the 40 S ribosome (11) and in the nucleus (12). Human LamR and Rps0, the homolog in yeast, which does not exhibit laminin binding activity, share 60% sequence identity (see Fig. 1). Rps0 is responsible for 20 S ribosomal RNA processing and maturation of the 40 S ribosomal protein subunit, directly affecting protein synthesis levels (13). Both the localization of human LamR to more than one intracellular component and the multiple functions of its homolog in yeast suggest that human LamR may also have numerous functions at the intracellular level.

## EXPERIMENTAL PROCEDURES

**Recombinant LamR Expression and Purification**—Residues 1–220 of human 37-kDa LamR precursor protein (LamR220) were subcloned from a full-length LamR cDNA into an *Escherichia coli* expression vector that includes a tobacco etch virus-cleavable, N-terminal His<sub>6</sub> tag. The construct was verified by automated DNA sequencing. The vector encoding LamR220 was transformed into *E. coli* strain BL21 (DE3\*), and cultures were grown in Luria broth medium at 37 °C to an A<sub>600</sub> of 0.6. Protein expression was induced by the addition of isopropyl-thiogalactopyranoside (0.1 mM) for 12 h at 20 °C. Cells were harvested, resuspended in lysis buffer (50 mM Tris (pH 8.0), 300 mM NaCl, 0.1% Triton X-100, 10% glycerol, EDTA-free protease inhibitor tablet (Roche Applied Science)), and lysed by French press. The lysate was centrifuged at 16,000 RPM for 30 min, and the supernatant was collected. The soluble fraction was purified by nickel-nitrilotriacetic acid chromatography (Qiagen) followed by gel filtration chromatography (Superdex 75, Amersham Biosciences). Protein was concentrated in spin concentrators (Amicon, Millipore).

**Crystallization and Data Collection**—Crystals of LamR220 were grown at 17 °C by the hanging-drop vapor diffusion method in drops containing a 1:1 (v/v) ratio of protein solution at 10 mg/ml and reservoir solution containing 17% (w/v) polyethylene glycol 10,000, 120 mM sodium citrate, 100 mM MES (pH 6.0), and 5% (w/v) polyethylene glycol 1,500. Crystals belong to the tetragonal space group P4<sub>3</sub>2<sub>1</sub>2 with unit cell dimensions of *a* = 75.69 Å, *b* = 75.69 Å, and *c* = 99.01 Å. Crystals were soaked briefly in crystallization buffer with 20% glycerol (v/v) and then flash-frozen in liquid nitrogen. There is one LamR220 molecule in the asymmetric unit with a solvent

\* This work was supported by U. S. Public Health Service Grants CA100687 and CA68498 (to D. M.) and by grants from the NCI, National Institutes of Health and the Department of Health and Human Services. Some of the authors have competing interests. Specifically, the contents of this study are being utilized for a patent. According to the rules and regulations of New York University School of Medicine, if this patent is licensed by a third party, some of the authors (D. M., S. H., K. J.) may receive benefits in the form of royalties or equity participation. The costs of publication of this article were defrayed in part by the payment of page charges. This article must therefore be hereby marked "advertisement" in accordance with 18 U.S.C. Section 1734 solely to indicate this fact.

The atomic coordinates and structure factors (code 3BCH) have been deposited in the Protein Data Bank, Research Collaboratory for Structural Bioinformatics, Rutgers University, New Brunswick, NJ (<http://www.rcsb.org/>).

<sup>§</sup> The on-line version of this article (available at <http://www.jbc.org>) contains two supplemental figures.

<sup>1</sup> The recipient of an Irma T. Hirsch-I-Monique Weill-Caulier Career Scientist Award. To whom correspondence may be addressed: Skirball Institute of Biomolecular Medicine, New York University School of Medicine, 540 First Ave., New York, NY 10016. Tel.: 212-263-8938; Fax: 212-263-8951; E-mail: hubbard@saturn.med.nyu.edu.

<sup>2</sup> To whom correspondence may be addressed: Dept. of Pathology, New York University School of Medicine, 550 First Ave., New York, NY 10016. Tel.: 212-263-5599; Fax: 212-263-8211; E-mail: daniel.meruelo@med.nyu.edu.

<sup>3</sup> The abbreviations used are: LamR, laminin receptor; MES, 4-morpholineethanesulfonic acid; BSA, bovine serum albumin; PDB, Protein Data Bank; EGCG, (–)-epigallocatechin-3-gallate.

content of 56%. Diffraction data were collected to a resolution of 2.15 Å at X29 at the National Synchrotron Light Source at Brookhaven National Laboratory. Data were processed with HKL2000 (14). A molecular replacement solution was found with AMoRE (15) using as a search model the structure of the *Archaeoglobus fulgidus* 30 S ribosomal protein S2p (PDB code 1V16, chain A) (16). Rigid body refinement, simulated annealing, and positional and *B*-factor refinement were performed with CNS (17) and Refmac (18). Coot was used for model building (19). According to PROCHECK (20), 95.4% of the residues have backbone torsion angles in most favored regions, and 4.6% have backbone torsion angles in additional allowed regions.

**In Vitro Binding Affinity for laminin-1**—LamR220 and full-length LamR (LamR295) binding affinity for laminin-1 were tested *in vitro*. White polystyrene enzyme-linked immunosorbent assay 96-well microplates, precoated with murine laminin-1 (New England Biolabs), were blocked overnight at 4 °C with blocking buffer (3.0% BSA, 0.1% sodium azide in phosphate-buffered saline). Wells were incubated with increasing concentrations of LamR220 or LamR295, which was nickel affinity-purified as described above for 1 h at 37 °C. Each well was washed three times with blocking buffer. Penta-His horseradish peroxidase conjugate (1:500) (Qiagen) was incubated for 2 h at room temperature, and wells were washed three times with blocking buffer. Substrate solution was added and incubated for ~15 min before reading, and fluorescent absorbance was detected at 490 nm on an enzyme-linked immunosorbent assay plate reader (EL<sub>x</sub>800, Biotek Instruments, Inc.). Controls for buffer alone and nonspecific protein, BSA (New England Biolabs), were also tested. Experiments were performed in triplicate. A binding curve and  $K_d$  were generated for LamR220 and LamR295. The  $K_d$  was calculated using a one-site binding hyperbola and the equation  $Y = B_{\max} \times X / (K_d + X)$ . Each group was tested in triplicate, and binding affinity was determined by normalizing to background fluorescence.

**In Vitro Sindbis Virus Vector Inhibition**— $3 \times 10^6$  BHK-55 cells were plated in a 12-well plate for 24 h in  $\alpha$ MEM (Cellgro) supplemented with 10% fetal bovine serum. Sindbis virus vector that expressed a luciferin reporter upon replication (multiplicity of infection = 100) was incubated with control protein (BSA, New England Biolabs), LamR220, or alone and rotated at room temperature for 1 h. Cells were washed with Optimum (Invitrogen), and 300  $\mu$ l of sample was added. Samples were incubated, rotating gently for 1 h at room temperature to allow Sindbis viral vector attachment. The supernatant was aspirated, cells were washed with phosphate-buffered saline, and 1 ml of medium was added. The cells were incubated overnight at 37 °C, and medium was aspirated the next day. 200  $\mu$ l of

unsupplemented medium and 200  $\mu$ l of luciferin substrate (SteadyGlo luciferase assay, Promega) were added. The cells were shaken vigorously for 15 min. The relative luciferase units, which correspond to infectivity of Sindbis virus vector, of each sample were read using a luminometer (Glomax 20/20, Promega). Experiments were performed in triplicate. A two-tailed Student's *t* test was performed ( $p < 0.05$ ) to determine statistical significance.

## RESULTS AND DISCUSSION

**LamR Expression, Purification, Crystallization, and Structural Determination**—To better understand the function of LamR and its interaction with binding partners, we sought to crystallize the human LamR precursor protein. To this end, several different-length constructs were overexpressed in *E. coli*, including residues 1–295 (full-length), residues 1–220, and residues 1–195. Of these, only the 220-residue version of

**TABLE 1**  
LamR220 data collection and refinement statistics (molecular replacement)

Data collection	
Space group	P4 <sub>3</sub> 2 <sub>1</sub> 2
Cell dimensions	
<i>a</i> , <i>b</i> , <i>c</i> (Å)	75.69, 75.69, 99.01
$\alpha$ , $\beta$ , $\gamma$ (°)	90.00, 90.00, 90.00
Resolution (Å)	50.0 (2.15) <sup>a</sup>
<i>R</i> <sub>sym</sub> or <i>R</i> <sub>merge</sub> (%)	14.4 (47.7)
1/ $\delta$ I	5.0 (4.0)
Completeness (%)	100 (100)
Redundancy	9.4 (9.7)
Refinement	
Resolution (Å)	50.0–2.15
No. of reflections	14762
<i>R</i> <sub>work</sub> / <i>R</i> <sub>free</sub> (%)	18.5/22.4
No. of atoms	1712
Protein	1563
Ligand/ion	0
Water	149
Average <i>B</i> -factor	21.8
r.m.s. <sup>b</sup> deviations	
Bond lengths (Å)	0.009
Bond angles (°)	1.22

<sup>a</sup> Values in parentheses are for highest resolution shell (2.25–2.15 Å).

<sup>b</sup> r.m.s., root mean square.

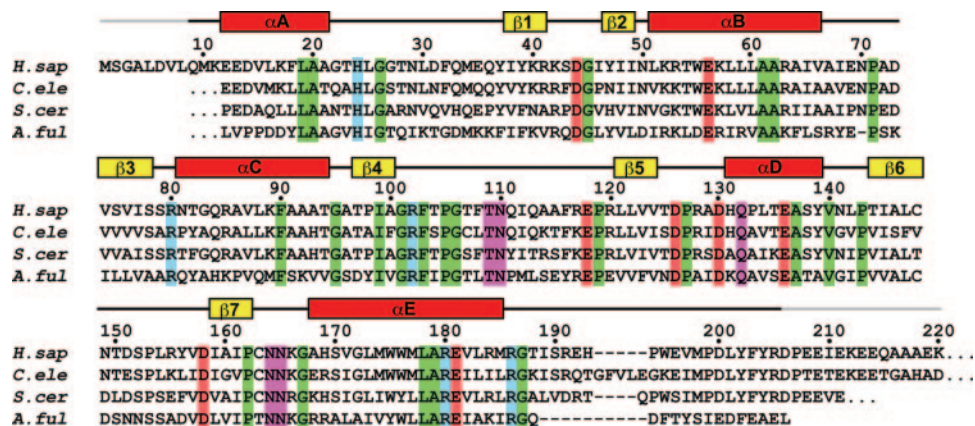


**FIGURE 1. Sequence homology between 37LRP/p40 orthologs.** *Homo sapiens* (*H. sap*) LamR (residues 1–220), *Caenorhabditis elegans* (*C. ele*) SA ribosomal protein (p40), *S. cerevisiae* (*S. cer*) S2p ribosomal protein, and *A. fulgidus* (*A. ful*) S2p ribosomal protein. Residue numbering is for human LamR. Conserved residue shading is as follows: red = acidic, blue = basic, green = hydrophobic, and magenta = hydrophilic. Secondary structure ( $\alpha$  helices, red;  $\beta$  strands, yellow) for LamR220 is shown according to PROCHECK (20). The gray lines indicate the N- and C-terminal portions of the structure that are disordered.

LamR (abbreviated LamR220) could be purified in amounts suitable for crystallization trials. LamR220 binds laminin-1 *in vitro* (supplemental Fig. 1*a*) and inhibits Sindbis virus vector infection of baby hamster kidney (BHK) cells (supplemental Fig. 1*b*). These data demonstrate that the first 220 residues of LamR are sufficient for interacting with key binding partners.

Crystals of LamR220 were obtained at pH 6.0 and belong to tetragonal space group  $P4_32_12$  with one molecule in the asymmetric unit. The crystal structure of LamR220 was determined by molecular replacement, using the crystal structure of the 30 S ribosomal protein S2p from *A. fulgidus* (PDB code 1V16) as a search model (16). Data collection and refinement statistics at 2.15 Å resolution are given in Table 1.

**Overall Structure of Human LamR**—Consistent with a sequence identity of 32% between LamR and *A. fulgidus* S2p (residues 15–183) (Fig. 1), the two proteins share a similar overall architecture, classified (Structural Classification of Proteins (SCOP)) as an  $\alpha/\beta$  protein with a flavodoxin-like fold (Fig. 2*a*). A central  $\beta$  sheet composed of five parallel  $\beta$  strands ( $\beta$ 3– $\beta$ 7) is flanked by three  $\alpha$  helices on one side ( $\alpha$ B,  $\alpha$ C, and  $\alpha$ E) and a single  $\alpha$  helix ( $\alpha$ D) on the other side. An N-terminal  $\alpha$  helix ( $\alpha$ A) and two anti-parallel  $\beta$  strands ( $\beta$ 1– $\beta$ 2) pack against the  $\alpha/\beta$  core of the protein. Residues 1–8 and 206–220 of LamR220 are disordered in the structure.

**Structural Comparison of Human LamR and S2 Protein from Other Species**—Superimposition of the structures of LamR220 and *A. fulgidus* S2p yields a root-mean-square deviation in  $C\alpha$  positions of just 0.9 Å (174 atoms) and reveals two areas in which the structures are divergent (Fig. 2*b*): a segment between  $\beta$ 4 and  $\beta$ 5 (residues 111–118 in LamR) and a segment after the last  $\alpha$  helix ( $\alpha$ E) (residues 188–196 in LamR), in which LamR contains a five-residue insertion relative to *A. fulgidus* S2p. The segment between  $\beta$ 4 and  $\beta$ 5 contains an equal number of residues in the two proteins. In *A. fulgidus* S2p, the segment is stabilized in a folded-back conformation via a salt bridge between Arg-113 in this segment (Arg-117 in LamR) and Asp-93 ( $\beta$ 4), the latter of which is not conserved in LamR (Thr-97). In the LamR220 structure, this segment instead projects away from the domain and packs against the same segment in a symmetry-

related (two-fold) molecule (Fig. 2*c*). In this crystallographic dimer, Ala-114 packs into a tight pocket in the symmetry-related molecule formed by the  $\beta$ 4– $\beta$ 5 segment and the end of  $\alpha$ D, and Phe-116 is in van der Waals contact with Tyr-139 ( $\alpha$ D) (Fig. 2*c*). Although Phe-116 is generally conserved from *Saccharomyces cerevisiae* through vertebrate species, Ala-114 is conserved only in vertebrates. The total surface area buried in this interface is a modest 832 Å<sup>2</sup>, and LamR220 runs as a monomer in solution, but in the context of a membrane attachment and a possible covalent dimerization linkage (9), this crystallographic dimer could be functionally significant.

**Functional Domains of LamR**—The structural differences noted between LamR220 and *A. fulgidus* S2p (Fig. 2*b*) could be important for ribosomal protein function or for the acquired function as the receptor for laminin. Analysis of the 3.0 Å res-

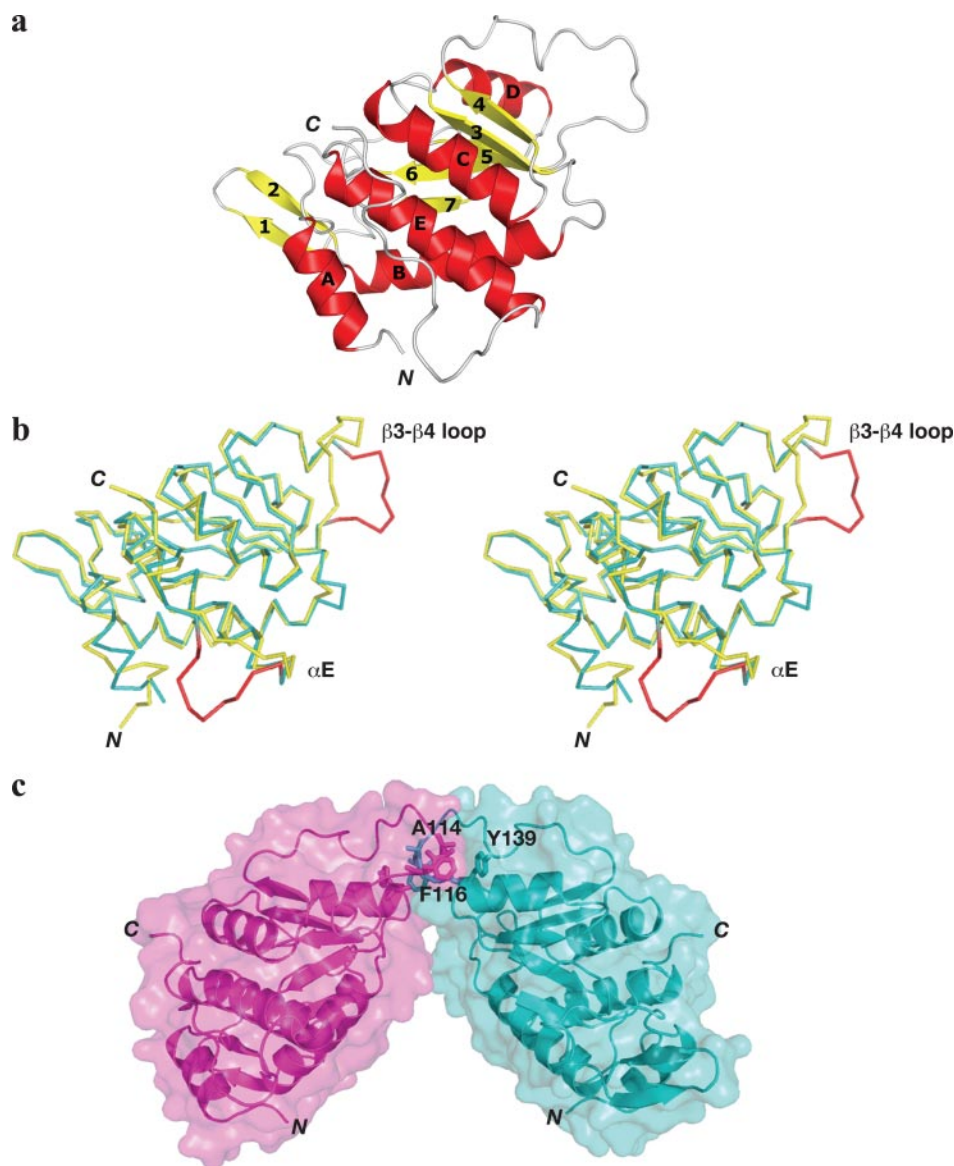


**FIGURE 2. Crystal structure of human LamR.** *a*, ribbon diagram of LamR220 with  $\alpha$  helices colored red and  $\beta$  strands colored yellow. *b*, superimposition of LamR220 (cyan) and *A. fulgidus* S2p (1V16) (yellow). Regions of divergence between the two structures are colored red in the LamR structure (residues 111–118 and 188–196). *c*, LamR220 dimer. One protomer is colored magenta, and the other is colored cyan. Residues in the dimer interface are labeled. The crystallographic two-fold axis is vertical.

olution structure of the 30 S ribosomal subunit from *Thermus thermophilus* (PDB code 1J5E) (21) indicates that the two major structural deviations between human LamR220 and *A. fulgidis* S2p (between  $\beta 4$  and  $\beta 5$  and after  $\alpha E$ ) would not appear to affect ribosomal function, since no RNA or protein contacts are present in these regions. This suggests that the structural differences in human LamR versus *A. fulgidis* S2p are important for laminin binding.

Previously, peptide segments of LamR utilized in binding assays implicated a segment, residues 161–180, known as peptide G, as a binding epitope for laminin (22). In the LamR220 crystal structure, this stretch of residues comprises the linker between  $\beta 7$  and most of  $\alpha E$ . The only portion of this sequence that is solvent-accessible are residues 165–169 in the  $\beta 7$ - $\alpha E$  linker. It is conceivable that the C-terminal tail of LamR220 undergoes a conformational change, exposing residues within this segment. Alternatively, the use of peptide segments of LamR to map the laminin binding site may need to be re-evaluated. In addition, a short putative transmembrane segment, residues 86–102, was suggested (22). This segment, encompassing  $\beta 4$  and most of  $\alpha C$ , is an integral part of the protein fold and is unlikely to serve as a transmembrane helix.

**Role of LamR in Disease**—LamR has been implicated in a variety of diseases, including neoplastic disorders, Creutzfeldt-Jacob disease, urinary tract infections, encephalitis, and others. In cancer, the specific inhibition of LamR function at the cell surface of tumor cells, either by binding of EGCG, which most likely competes with endogenous laminin, or by infection with Sindbis virus vector, which is internalized by receptor-mediated endocytosis, has been associated with anti-tumor effects (23–26). Both EGCG and Sindbis virus vectors, through two different mechanisms, reduce the ability of LamR at the surface to interact with laminin. The structural characterization of LamR will contribute to an understanding of how LamR interacts with its binding partners and aid in the development of therapeutics that can block and/or mimic LamR interactions in the setting of cancer, neurological disorders, and viral infection.

**Acknowledgments**—We thank Dr. Christine Pampeno and Dr. Jen-Chieh Tseng for critical reading of this manuscript and helpful discussions and Dr. Vivian Stojanoff for help in data collection at NSLS beamlines X6A and X29, Brookhaven National Laboratory, for which financial support comes principally from the Offices of Biological and Environmental Research and of Basic Energy Sciences of the U. S. Department of Energy and from the National Center for Research Resources of the National Institutes of Health.

## REFERENCES

- Jackers, P., Minoletti, F., Belotti, D., Clause, N., Sozzi, G., Sobel, M. E., and Castronovo, V. (1996) *Oncogene* **13**, 495–503
- Ardini, E., Pesole, G., Tagliabue, E., Magnifico, A., Castronovo, V., Sobel, M. E., Colnaghi, M. I., and Menard, S. (1998) *Mol. Biol. Evol.* **15**, 1017–1025
- Rao, N. C., Barsky, S. H., Terranova, V. P., and Liotta, L. A. (1983) *Biochem. Biophys. Res. Commun.* **111**, 804–808
- Gauczynski, S., Peyrin, J. M., Haik, S., Leucht, C., Hundt, C., Rieger, R., Krasemann, S., Deslys, J. P., Dormont, D., Lasmezas, C. I., and Weiss, S. (2001) *EMBO J.* **20**, 5863–5875
- Wang, K. S., Kuhn, R. J., Strauss, E. G., Ou, S., and Strauss, J. H. (1992) *J. Virol.* **66**, 4992–5001
- Ludwig, G. V., Kondig, J. P., and Smith, J. F. (1996) *J. Virol.* **70**, 5592–5599
- McNichol, B. A., Rasmussen, S. B., Carvalho, H. M., Meysick, K. C., and O'Brien, A. D. (2007) *Infect. Immun.* **75**, 5095–5104
- Akache, B., Grimm, D., Pandey, K., Yant, S. R., Xu, H., and Kay, M. A. (2006) *J. Virol.* **80**, 9831–9836
- Landowski, T. H., Dratz, E. A., and Starkey, J. R. (1995) *Biochemistry* **34**, 11276–11287
- Menard, S., Tagliabue, E., and Colnaghi, M. I. (1998) *Breast Cancer Res. Treat.* **52**, 137–145
- Auth, D., and Brawerman, G. (1992) *Proc. Natl. Acad. Sci. U. S. A.* **89**, 4368–4372
- Sato, M., Kinoshita, K., Kaneda, Y., Saeki, Y., Iwamatsu, A., and Tanaka, K. (1996) *Biochem. Biophys. Res. Commun.* **229**, 896–901
- Ford, C. L., Randal-Whitis, L., and Ellis, S. R. (1999) *Cancer Res.* **59**, 704–710
- Otwinowski, Z., and Minor, W. (1997) *Methods Enzymol.* **276**, 307–326
- Navaza, J. (1994) *Acta Crystallogr. Sect. A* **50**, 157–163
- Badger, J., Sauder, J. M., Adams, J. M., Antonyamy, S., Bain, K., Bergseid, M. G., Buchanan, S. G., Buchanan, M. D., Batiyenko, Y., Christopher, J. A., Emtage, S., Eroshkina, A., Feil, I., Furlong, E. B., Gajiwala, K. S., Gao, X., He, D., Hendle, J., Huber, A., Hoda, K., Kearins, P., Kissinger, C., Laubert, B., Lewis, H. A., Lin, J., Loomis, K., Lorimer, D., Louie, G., Maletic, M., Marsh, C. D., Miller, I., Molinari, J., Muller-Dieckmann, H. J., Newman, J. M., Noland, B. W., Pagarigan, B., Park, F., Peat, T. S., Post, K. W., Radojicic, S., Ramos, A., Romero, R., Rutter, M. E., Sanderson, W. E., Schwinn, K. D., Tresser, J., Winhoven, J., Wright, T. A., Wu, L., Xu, J., and Harris, T. J. (2005) *Proteins* **60**, 787–796
- Brunger, A. T., Adams, P. D., Clore, G. M., DeLano, W. L., Gros, P., Grosse-Kunstleve, R. W., Jiang, J. S., Kuszewski, J., Nilges, M., Pannu, N. S., Read, R. J., Rice, L. M., Simonson, T., and Warren, G. L. (1998) *Acta Crystallogr.* **54**, 905–921
- Murshudov, G. N., Vagin, A. A., and Dodson, E. J. (1997) *Acta Crystallogr.* **53**, 240–255
- Emsley, P., and Cowtan, K. (2004) *Acta Crystallogr.* **60**, 2126–2132
- Laskowski, R. A., MacArthur, M. W., Moss, D. S., and Thornton, J. M. (1993) *J. Appl. Crystallogr.* **26**, 283–291
- Wimberly, B. T., Brodersen, D. E., Clemons, W. M., Jr., Morgan-Warren, R. J., Carter, A. P., Vornrhein, C., Hartsch, T., and Ramakrishnan, V. (2000) *Nature* **407**, 327–339
- Castronovo, V., Tarabozetti, G., and Sobel, M. E. (1991) *J. Biol. Chem.* **266**, 20440–20446
- Tanaka, M., Narumi, K., Isemura, M., Abe, M., Sato, Y., Abe, T., Saijo, Y., Nukiwa, T., and Satoh, K. (2000) *Cancer Lett.* **153**, 161–168
- Tachibana, H., Koga, K., Fujimura, Y., and Yamada, K. (2004) *Nat. Struct. Mol. Biol.* **11**, 380–381
- Tseng, J. C., Levin, B., Hurtado, A., Yee, H., Perez de Castro, I., Jimenez, M., Shamamian, P., Jin, R., Novick, R. P., Pellicer, A., and Meruelo, D. (2004) *Nat. Biotechnol.* **22**, 70–77
- Cao, Y., and Cao, R. (1999) *Nature* **398**, 381